Argonne NATIONAL LABORATORY

Intra-Laboratory Memo

November 8, 2010

TO: **James E. Matos**

FROM: **Earl E. Feldman and M. Kalimullah**

SUBJECT: **Steady-State Thermal-Hydraulic Analysis for Natural-Convective Flow in the Rhode Island Nuclear Science Center (RINSC) Reactor**

4.7 Steady-State Natural Convection

4.7.1 Limits

For operation in the natural-convective mode, the recently revised RINSC reactor Technical Specifications provide Safety Limit values for power of 200 kW, a peak coolant inlet temperature of 130° F, and a minimum pool water depth of 23 feet 6.5 inches (23.54 feet) above the active core. These extreme true values, which are not to be violated under any circumstances, are to be compared with the corresponding LSSS values of 115 kW, 125° F, and 23 feet 9.6 inches and the corresponding Limiting Trip values of 125 kW, 128° F, and 23 feet 9.1 inches. The analysis will show that operation at the Safety Limits will not cause fuel damage.

4.7.2 Flow Paths

During natural-convective operation the primary pumps are off. Since the flow through the core is driven by buoyancy, the flow direction is upward instead of the normal forced-flow downward direction. For the natural-convective mode of operation, the flow going to the reactor core is drawn from the pool and follows the path indicated by the red arrows in Figure 4.7-1 to the bottoms of the fuel assemblies. After the flow exits the tops of the assemblies it goes directly back to the pool because the top of the core box is open to the pool. Since the primary flow circulates between the pool and the core and does not pass through a heat exchanger, heat produced in the primary system is not removed by a secondary-loop flow. Thus, the pool gradually heats up. Operation is stopped before the measured pool temperature reaches the LSSS value.

During normal steady-state operation in the forced-convection mode, the operating primary pump applies a suction to the lower plenum (or discharge header) and the outlet pipe. As shown just ahead of the leftmost red arrow in Figure 4.7-1, there is a vertical rectangular window in the outlet duct that is 6 inches wide and 12 inches high that is covered by the coolant header gate during normal steady-state operation. When the primary flow drops below 1000 gpm, a counterweight (in the form of a paddle in the flow stream) causes the gate to open. The gate is on the outside of the duct and is hinged from the top about 2 inches above the window opening. The paddle in the flow stream, as shown in the figure, is rigidly attached to the gate. During normal forced-flow operation, the flow pushes against the paddle which, along with the suction in the duct, holds the gate tightly against the window. Because of the manner in which the gate is hinged and counterweighted, the gate may only open about 30° during operation in the natural-convective mode. However, this is sufficient for the total flow area between the open gate and the vertical face of the duct to be about twice that of the flow area of the rectangular window.

During operation in the natural-convective mode, coolant from the pool directly enters the outlet duct, which becomes an inlet duct. The hydraulic resistance along the path indicated by the red arrows in Figure 4.7-1 can significantly affect the flow rate through the core. Therefore, this hydraulic resistance must be included in the hydraulics model. Because the core box is open to the pool at the top, the flow exiting the fuel assemblies can return to the pool without passing through any of the ductwork that normally provides flow to the core top during normal forced-flow operation.

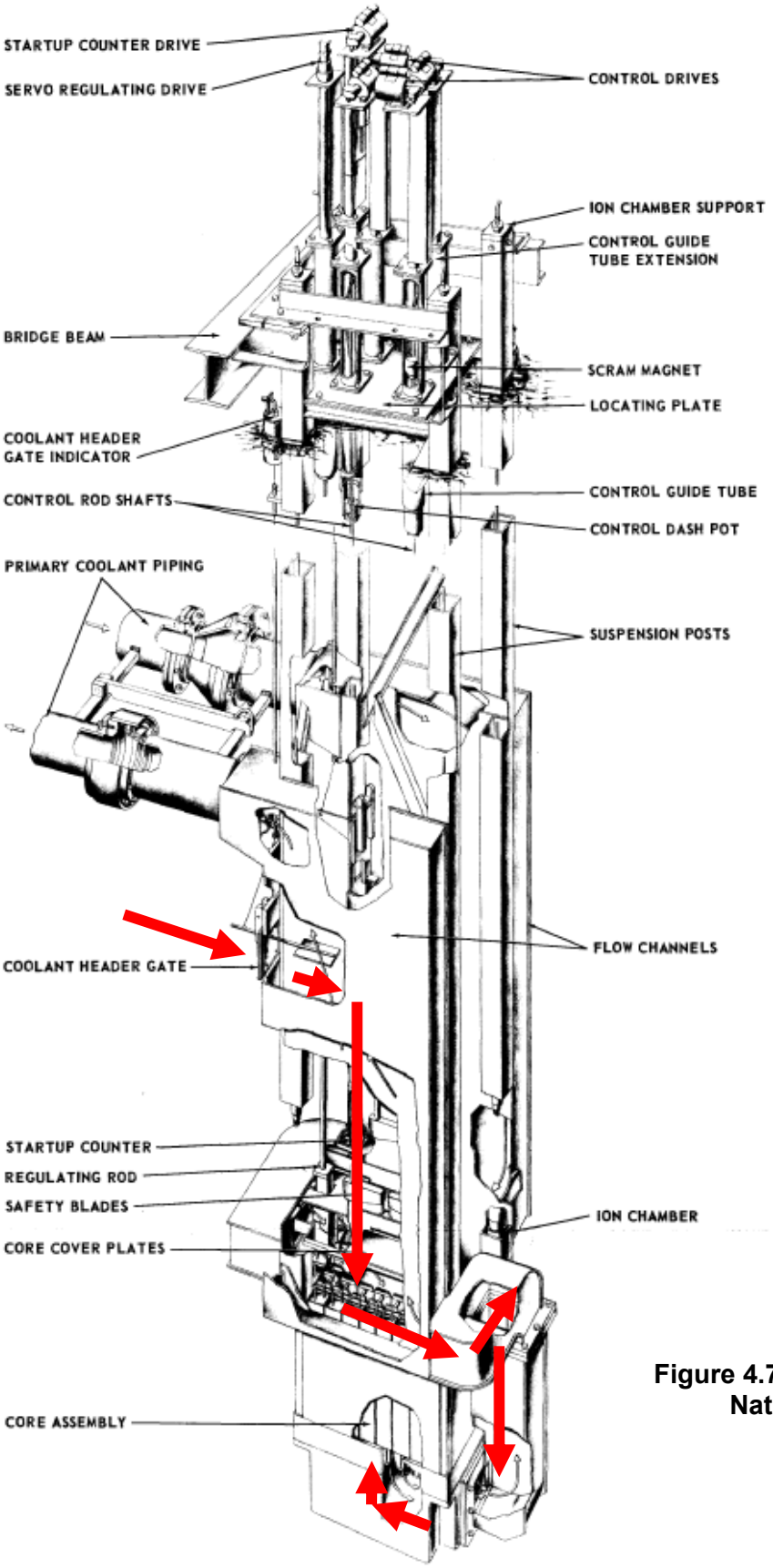

Figure 4.7-1 Inlet Flow Path for Natural Convection

4.7.3 Hydraulic Resistance from the Pool to the Assembly Inlet

The following General Electric drawings were used in estimating the dimensions of the ducts connecting the window in the outlet duct to the lower plenum:

1. 198E264 – Assembly Frame - Suspension
2. 197E251 – Assembly Frame and Header
3. 198E261 – Core Support Arrg't
4. 693C915 – Gate

The first two drawing show much of the ductwork. The third drawing shows the core box, grid plate, and lower plenum assembly. The lower plenum, which is labeled "discharge header" in the third drawing, connects to the bottom of the grid plate. The distance from the bottom of the grid plate to the lower exterior surface of the plenum is 16 inches. The fourth drawing just shows a gate. The first three are complex assembly drawings with multiple top, side, bottom, and cut-away views. These drawings do not provide all of the detailed dimensions needed to fully describe the inlet path. However, there are enough dimensions to deduce duct sizes, at least approximately, and are sufficient for estimating hydraulic resistances.

Table 4.7-1 shows the approximate dimensions that were deduced from the four drawings listed above. The seven items in the table occur in sequence starting at the gate opening and ending at the lower plenum. Item no. 1 in the table is the window area, which is located in one of the two thin vertical sides of the long thin vertical duct, item no. 2. Items 2, 4, and 6 are the three ducts that are connected in series along the entire length of the path to the lower plenum. Item no. 3 is the vertical plane where the long thin vertical duct intersects the horizontal duct (item no. 4) along the side of the core box. Item no. 5 is the horizontal plane where the horizontal duct meets the vertical duct (item no. 6) that connects to the side of the lower plenum. The flow areas in the inlet path are important because pressure drop is proportional to the square of velocity.

The flow areas, which are provided in the table, should to be compared to the core flow area of the fueled channels. Table 4.6-5 shows the flow areas for the 312 (294 + 10 + 7 + 1) fueled channels. Based on the values in Table 4.6-5, the total combined flow area of the fueled channels in the core is 72.4 in^2. As the last column in Table 4.7-1 shows, the flow areas of the inlet path are about the same as the core fueled flow area or larger. Table 4.7-1 also shows that the hydraulic diameter of each part of the inlet path is about 10 inches. Thus, each segment of the inlet flow path is no more than several hydraulic diameters long. Hence, most of the hydraulic resistance is due to form and turning, i.e, K-losses, rather than due to wall friction.

Since the minimum flow area in the inlet path of 72 in^2 is essentially the same as the core flow area of the fueled channels of 72.4 in^2, the velocity at the inlet to an average coolant channel should be about the same as the maximum velocity in the inlet flow path. Therefore, in the modeling with the PLTEMP/ANL code, the inlet path hydraulic resistance will be represented as a K-loss at the inlet to the channel.

The pressure drop in the inlet flow path is the sum of a series of pressure drops, which are each represented by $K_i \times \rho \times V_i^2/2$, where ρ is the coolant density, K_i is the form or turning resistance

factor for the i^{th} resistance, and V_i is the flow velocity associated with the i^{th} resistance. As is standard practice, where there is a pressure drop due to a change in flow area, V_i is the velocity of the smallest of the areas.

Table 4.7-1 Inlet Path

No.	Path Segment or Opening	V*	H*	D*	Flow Area, in^2	Wetted Perimeter, in	Hydraulic Diameter, in	Area Ratio**
1	Gate opening	12	6		72	36	8	0.99
2	Thin wide long vertical duct		29.5	6	177	71	10	2.44
3	Vertical plane where no. 2 meets no. 4	12		6	72	36	8	0.99
4	Horizontal duct along top of core box	12		9	108	42	10.3	1.49
5	Horizontal plane where no. 4 meets no. 6		9	9.625	86.6	37	9.3	1.20
6	Vertical duct to lower plenum		9	~10	90	38	9.5	1.24
7	Opening in the side of outlet plenum	12	9		108	42	10.3	1.49

*Duct or opening linear dimension in inches, where V is the vertical direction, H is in the horizontal direction along the side of the core box, and D is the depth direction perpendicular to the side of the core box.
**Ratio of flow area to total fueled channel flow area of 72.4 $inches^2$.

Books, such as Reference 1, provide values of K-loss for a variety of flow situations. However, nothing in these books can closely match the details in the inlet flow path of the RINSC reactor. Also, specific dimensions and details for the inlet path are not available. Even if all of these details were know, only an experimental measurement would be capable of providing an accurate value for an effective K value to apply to the average fuel channel inlet to represent the overall inlet path hydraulic resistance. However, each segment of the inlet path can be examined and a conservatively large value of the K_i value for each will be used. This will result in a conservatively large value of the overall K. The sensitivity of the margin to the onset of nucleate boiling to the overall K value will be studied to provide confidence in the results and to show that excessive conservatism is not leading to erroneously excessively limiting predictions of thermal performance.

Diagram 4-12 of Reference 1 shows the K value for a duct of flow area F_1, passing through an orifice of area F_0, into a duct of area F_2. Based on this with F_1 infinite, F_0 at 72 in^2, and F_2 at 177 in^2, it is estimate that the overall K-loss from the pool, through the gate and into the thin wide long vertical duct is 1.4. Since the minimum area here is F_0, which is 72 in^2 and essentially the same as the 72.4 in^2 area of the core, no adjustment is needed to relate this K-value to the average core inlet velocity. After entering the thin long vertical duct, the flow makes two 90° turns, one from the horizontal direction to the vertically downward direction and a second one from the vertically downward direction back to the horizontal direction. Each of these will be assigned a K value of 1.0. However, since the flow area is 2.44 times as big as the core flow

area, the K loss value should be divided by a factor of 2.44^2. Therefore, the adjusted K-value is $(1 + 1)/2.44^2 = 0.3$.

The flow next exits the thin wide long vertical duct and enters the horizontal duct along the top of the core box. Diagram 4-12 of Reference 1 is used again, but this time it is used to represent the passage from one duct segment into the next with $F_1 = 177$ in^2, $F_0 = 72$ in^2, and $F_2 = 108$ in^2. This leads to a K-value of 0.9. As in the previous application of Diagram 4-12, F_0 is 72 in^2 and no adjustment is needed to relate this K-value to the average core inlet velocity. There are three 90° turns in the rest of the approximately square ductwork that connects the thin wide long vertical duct to the side inlet to the lower plenum. Each of these will be assumed to have a K-value of 1. No reduction in this K-value will be taken due to the approximately square duct flow areas being somewhat bigger than the core flow area. The final expansion from the approximately square ductwork into the side of the lower plenum will be assigned a K-value of 1.0, which is what it would be for an infinite expansion with no reduction taken due to the duct flow area being greater than the core flow area. Since the lower plenum flow area is extremely large compared to the core flow area, the turning loss within the plenum from the horizontal to the vertical direction is negligibly small. Thus, the overall K value is 1.4 + 0.3 + 0.9 + 3 + 1 = 6.6. This will be rounded up to 10.0 for the analysis.

As shown in Table 4.6-5, for downward flow there is a total K value of 1.048 within each assembly due to a flow contraction going into the fuel plate region, a flow expansion coming out of the fuel plate region, a flow contraction going into the lower end box, and a flow expansion coming out of the lower end box. When the flow direction is reversed, the contraction and expansion for the end box precedes the contraction and expansion for the fuel plate region, but the same area ratios apply to each region. The same total K loss would result for upward flow as for downward if the Reynolds number were above 10,000 for the upward direction as it is for the downward direction. However, for natural convection at a core power of 200 kW, the Reynolds number in the fuel region is about 500 to 700 and close to 10,000 in the lower end box. The larger Reynolds number for the lower end box is due to the hydraulic diameter being a few inches there, which is much larger than the 0.17-inch hydraulic diameter between internal fuel plates of the same assembly. These Reynolds numbers are not known a priori and must be verified from the analytical results below.

As Diagrams 4-10 of Reference 1 indicates, for a Reynolds number of 500, the K-loss value for the contraction into the fuel would be less than twice as big as the 0.275 values shown in Table 4.6-5 Similarly, a sudden expansion in the laminar flow region is expected to produce a K-loss value that is no more than a few times larger than it would be for turbulent flow. Thus, the lower Reynolds numbers for laminar natural-convective flow could result in an overall K-loss value within the fuel assemblies that is perhaps twice as large as 1.048 assumed for the force-convection analysis. Since the increase is small compared to the resistance in the ductwork leading to the lower plenum, it will be ignored. The 1.048 value use for the force-flow overall K-loss will be rounded off to 1.0 and split equally between the core inlet and outlet. Thus, a total K value of 11.0 will be used in the analysis, with 10.5 at the inlet and 0.5 at the outlet.

It will be shown below that a wide range of assumed values of inlet ductwork K-loss values from double the conservative value assumed in the analysis down to zero will affect the power margin

to onset of nucleate boiling by only several percent in either direction relative to the nominal conservative value assumed in the analysis. The reason for the relative insensitivity to inlet piping K-loss value is that the coolant channel wall friction – which is represented by friction factor times channel length divided by channel hydraulic diameter – is large compared to the inlet piping K-loss value. The coolant channel wall friction value, which is typically on the order of 20, is relatively large because the flow is laminar rather than turbulent in the coolant channels. As shown in Table 4.6-5 for a 1580 forced-convective flow in the fueled paths, the corresponding values for turbulent flow are between 3.2 and 5.1.

An important assumption in estimating the inlet path overall K value for natural convection is that the flow in the ductwork leading to the lower plenum is turbulent. If the flow there were not turbulent, then the overall K value for the ductwork could be significantly greater than indicated above and a function of Reynolds number. That the flow in the inlet duct is turbulent is easy to verify once an approximate value for the total flow rate through the core, which is the same as the flow through the duct leading to the lower plenum, is determined. Also, the flow solution will be used to show that for an assumed reactor power of 200 kW, the Reynolds number in the flow channels is about 500 to 700, as indicated above.

4.7.4 Thermal-Hydraulics Model for Natural Convection

4.7.4.1 Modeling Fundamental

The only mechanism pushing the flow upward through the core is buoyancy. This buoyancy is due to the warmer coolant temperatures in the core relative to those of the open pool. The fuel plate length is the same 25.0-inch length used in the thermal analysis of forced convection. The 23.25-inch long fuel meat is centered in this length with 0.875 inches above and 0.875 inches below the fuel meat. There is no additional chimney assumed although a case could be made for it. There is an end box at the top of each assembly, which is identical to the one at the bottom, which could serve as a chimney. Also, the vertical distance from the top of the fuel plates to the open pool above the core box is at least a foot. However, the flows from individual channels and from the pool can mix in this region, making the benefit of the added chimney effect difficult to assess accurately.

The core flow rate is determine in the model by balancing the buoyancy- induced pressure rise in the core with the friction and K-loss pressure drops through the core combined with the sum of the K-loss pressure drops through the ductwork from the coolant header gate to the core inlet.

In the analysis, as in the analysis of forced-convective flow, only the limiting channel will be modeled. The PLTEMP/ANL model used to analyze forced flow is adapted for natural-convective flow. However, because of the tight coupling between the buoyancy-induced flow and core coolant temperatures, the flow rate must be determined by the PLTEMP/ANL model rather than with a separate independent hydraulics model, such as the one use for forced-convective flow..

4.7.4.2 Single-Plate Limiting-Channel Model

The limiting location is channel 2 and plate 1 of assembly D6 as indentified in Table 4.6-8. This is represented in the PLTEMP/ANL analysis as plate 1 cooled on each side by a half of a symmetric 0.088-inch thick internal coolant channel, as was done for the analysis of forced convection. The axial power shape is as shown in Figure 4.6-5 except that axial location 1.0 is the bottom of the fuel meat and axial location 0.0 is the top of the fuel meat. Obviously, if the ordinate were relabeled for analysis of natural convection it would read "Relative Distance from the Top along the Fuel Meat Length". In the PLTEMP/ANL input file the axial power shape was inverted because the code expects the power shape to be listed from the inlet to the outlet.

The pool and core inlet temperature is taken to be the safety limit value of 130° F, which is 5° C greater than the LSSS value.. The core pressure at the top of the core is based on the pool level being at its safety limit value of 23.54 feet above the active core. The density of 130° F water is 986.0 kg/m^3. Analogous to the analysis in the first paragraph of Section 4.6.5, the added pressure at the top of the fuel due to the weight of the water is 0.694 bar and the total pressure is 1.707 bar. The inlet to the fuel plates is 23.25 + 7/8 inches below the top of the fuel meat. This added distance adds 0.059 bar to the inlet pressure. For natural-convective flow the friction pressure drop is about two orders of magnitude smaller than this value. Thus, the pressure at the bottom of the fuel plates is taken to be 1.75 bar.

4.7.4.3 Adjusting the Inlet Piping K-loss So That It Can Be Used with the Limiting Channel Rather Than the Average Channel

In the PLTEMP/ANL model of the highest power plate in the core, the combined flow rate through the two-half channels on either side of the plate will be considerably greater than that for the similar two-half channels on either side of the average-power plate. This is because the much higher than average coolant temperatures in the limiting channel will induce much more buoyant flow through the limiting channel than through an average-power channel. Thus, the inlet velocity associated with the highest power plate will be much greater than that associated with the average plate. However, the flow in the ductwork leading to the lower plenum corresponds to the average core velocity (i.e., the total core flow rate divided by the total fueled region flow area), not the velocity in the hottest channels. As shown in Table 4.6-8 for operation at 2.0 MW, the hottest plate is the first plate of Assembly D6, which has a plate power of 9.653 kW. For 200-kW operation, corresponding plate power is one-tenth as large, or 0.9653 kW. Since there are 308 plates in the core, the average plate produces 200 kW / 308 = 0.6494 kW.

Two PLTEMP/ANL cases were developed to study the difference between the flow rates in the limiting and average channels. The single-plate limiting channel model was solved for a fuel plate power of 0.9653 kW. All of the hot channel factors were set to 1.0 except for a global hot channel factor on film coefficient, which was set to 1.2, the same value that was used for force-flow analysis. The inlet K-loss was assumed to be 10.5 and the exit K-loss was assumed to be 0.5, as discussed earlier. The PLTEMP/ANL solution yielded a combined flow for the two half channels on either side of the fuel plate of 8.19×10^{-3} kg/s. The second PLTEMP/ANL case was the same as the first except that the plate power was reduced to 0.6494 kW. The resultant combined flow for the two half channels was 6.75×10^{-3} kg/s.

Since pressure drop in the inlet duct is proportional to flow rate squared, it is estimated that the K-loss value of 10 for the inlet ductwork should be reduced by a factor of $(6.75 \times 10^{-3} / 8.19 \times 10^{-3})^2 = 0.68$ to 6.8. Therefore, when the highest power plate is analyzed with the PLTEMP/ANL model, the K-loss value of 10, which represents the resistance in the ductwork, will be reduced to 7. Thus, the total inlet K-loss of 7.5 will be used and the outlet K-loss will remain at 0.5.

The lack of precision in determining the adjustment to the K-loss is not a major concern because, as indicated above, it will be shown below that the margin to onset of nucleate boiling is relatively insensitive to the value of inlet piping K-loss value.

4.7.4.4 Estimating Channel and Inlet Duct Reynolds Numbers

The second of the above two PLTEMP/ANL cases showed that an internal channel with the average plate power 0.6494 kW produced a flow rate of 6.75×10^{-3} kg/s. As Table 4.6-5 shows, there are 294 internal channels and only 18 other fueled channels. The combined flow through the 294 internal channels is estimated to be 294 times the flow through the average channel calculated above with PLTEMP/ANL with a ductwork K-loss of 10 and a channel power of 0.6494 kW, or $294 \times 6.75 \times 10^{-3}$ kg/s = 1.98 kg/s. The total core flow must be greater than this value. The Reynolds number is the product of the density, velocity, and hydraulic diameter divided by the viscosity. It is easily to show that this is mathematically equal to 4 times the flow rate divided by the product of the viscosity and the wetted perimeter. The viscosity of the water at the inlet is 0.0005081 Pa-s. As shown in Table 4.7-1, the wetted perimeter is between 36 and 71 inches. Thus, the lowest value of duct Reynolds number is at least 4 × 1.98 kg/s / (0.0005081 Pa-s × 71 inches × 0.0254 m/inch) = 8643, which is clearly in the turbulent range, which starts at about 2200 or 2300. For two of the K-loss components of the ductwork leading to the lower plenum where Diagram 4-12 of Reference 1 was used, a Reynolds number greater than 10,000 at the minimum of the three flow areas in Diagram 4-12 was required. For each of these two instances the minimum flow area was 72 $in.^2$ and the wetted perimeter was 36 inches. Thus, the Reynolds number at these locations is at least 4 × 1.98 kg/s / (0.0005081 Pa-s × 36 inches × 0.0254 m/inch) = 17,047, which is greater than 10,000.

An additional PLTEMP/ANL analysis was performed in order to estimate the Reynolds numbers in the limiting coolant channel. For this analysis, the PLTEMP/ANL analysis of the hottest plate was repeated, but with the K-loss value representing the inlet duct reduced from 10 to 7. Thus, in the PLTEMP/ANL model the total inlet K-loss value was 7.5 and the outlet one was 0.5. The reduction in the inlet K-loss value caused the flow rate in the limiting channel to increase by only 3.7 %. For this case, the PLTEMP/ANL output shows that the coolant channel Reynolds number is 503 at the inlet and increases monotonically to 706 at the outlet. Thus, the flow inside the heated channels is laminar. The increase in Reynolds number along the length is due to a decrease in viscosity with increasing coolant temperature. This additional PLTEMP/ANL analysis has an input file name of NatConv_RI_200kW_03b.inp and represents the based case that is used below in perturbation studies to obtain hot channel factors.

4.7.4.5 Hot Channel Factors

The table of hot channel factors used for the forced-flow analysis, Table 4.6-7, is used as a starting point for the creation of a hot channel factor table for natural convection, Table 4.7-2. The uncertainty/error due to flow distribution does not apply to natural-convective flow and is not included. In forced convection there is a fixed amount of flow that is measured and distributed among all of the coolant channels in the core. In natural-convective flow, the total core flow is not fixed and more flow going to one channel does not imply that less flow goes to another. Similarly, since there is no flow measurement, there is no flow measurement error. Thus, this uncertainty/error is also not included in Table 4.7-2.

The global or systematic errors on core power and film coefficient are treated the same as for forced flow. This film coefficient error is assumed to be 20%, as was assumed for forced flow. In the table, as in the forced-flow case, because the power measure error is included in the interpretation of the results, the tolerance fraction for power measurement is set to 0 and the hot channel factor for power measurement is set to 1.0. As shown in Chapter 14, section 2.2.2, the safety limit value is 200 kW. This is a true value (as opposed to a measured value) that must not be exceeded under any circumstances during the natural-convective mode of operation. Chapter 14, section 2.2.2, also indicates that the corresponding nominal power is 100 kW, the LSSS value is 115 kW, the measurement error is taken to be 10% of. 100 kW, or 10 kW. Thus, the limiting trip value (at the LSSS) could be as high as 125 kW, which leaves a 75 kW margin to the 200 kW safety limit value.

The first two hot channel factor uncertainty items in Table 4.7-2, "fuel meat thickness (local)" and "U235 homogeneity (local)", behave in the same manner and have the same values as in the forced-flow case. Because these affect only local heat flux and have no effect on bulk coolant temperature, they do not affect the buoyancy-driven flow.

The next two items in the table, "U235 loading per plate" and "power density", do affect bulk coolant temperature and buoyancy-drive flow. Their hot channel factors for heat flux, F_q, and film temperature rise, F_{film}, are the same as indicated in Table 4.6-7. The reason that F_{film} is not influenced by the buoyancy-driven flow rate is because in laminar flow the Nusselt number is constant and not a function of flow rate. The beneficial effect of the increase in buoyancy-driven flow on the channel flow rate hot channel factors, F_w, will be ignored. To include it would require hot channels factor that are less than 1.0. The values of channel temperature rise hot channel factors, F_{bulk}, for "U235 loading per plate" and "power density" will be determined by a perturbation method.

The base case, as identified above, has PLTEMP/ANL input file name "NatConv_RI_200kW_03b.inp". The perturbed case is the same as the base case except that the power into the channel was increased by 5% for the "power density" uncertainty case. The bulk coolant temperature rise increased from 27.066° C in the base case to 27.739° C in the perturbed case. Thus, although the power increased by 5%, the bulk coolant temperature rise increased by only 2.487%. This is less than 5% because the increase in buoyancy caused the flow rate to increase from 8.4960×10^{-3} kg/s to 8.7042×10^{-3} kg/s for the two half channels combined, or 2.452%. Based on a these two cases, the 0.10 power fraction for power density yields a 1.025

Table 4.7-2 – Hot Channel Factors for Natural-Convective Flow

					hot channel factors			
uncertainty	effect on bulk ΔT, fraction	value, inches or mm	toler-ance, inches or mm	toler-ance, fraction	heat flux, F_q	channel flow rate, F_w	channel temper-ature rise, F_{bulk}	film temper-ature rise, F_{film}
random errors	-							
fuel meat thickness (local)				0.00	1.00			1.00
U235 homogeneity (local)				0.20	1.20			1.20
U235 loading per plate	0.50			0.03	1.03		1.007	1.03
power density	0.50			0.10	1.10		1.025	1.10
channel spacing	1.00	0.088	0.006	1.073		1.064	1.064	1.00
random errors combined					1.23	1.06	1.07	1.23
systematic errors								
power measurement	1.00			0.00	1.00		1.00	1.00
heat transfer coefficient				0.20				1.20
systematic errors combined					1.00	1.00	1.00	1.20
product of random & systematic combinations					1.23	1.06	1.07	1.48

F_{bulk} hot channel factor component. The 0.03 tolerance fraction on U235 fuel plate loading is estimate to produce a proportional F_{bulk} hot channel factor component of $1 + 0.03/0.10 \times 0.02487 = 1.007$.

In the above perturbation analysis there is a subtle beneficial effect that we choose to ignore. The model of the perturbed channel assumes that the flow and pressure drop in the inlet duct leading to the lower plenum is increased along with the limiting channel flow. This is not true since the total core power is not increased at all. Increasing the power in one fuel plate causes other plates to produce less power, since the total reactor power is controlled and constant. Thus, the flow rate in the perturbed case would be slightly greater than predicted because the inlet duct pressure drop does not increase, as required in the perturbed case. Thus, the perturbed bulk coolant temperature rise would be slightly less than predicted and the hot channel factor would be slight smaller. In any case, this beneficial effect is extremely small.

The last uncertainty/error to be considered in Table 4.7-2 is the one due to channel spacing uncertainty. The channel thickness for the internal channel of each assembly is 88±6 mils. It is not obvious that decreasing the channel thickness from its nominal value of 88 mils to its minimum of 82 mils will result in a smaller margin to the onset of nucleate boiling. Nucleate boiling is based on the peak clad surface temperature. Reducing the channel thickness causes two opposing effects. The adverse effect is reduced flow, which increases the bulk coolant temperature. The beneficial effect is an increase in film coefficient which reduces the film temperature rise from the bulk coolant to the clad surface. Because the flow is laminar, the Nusselt number is a constant. By definition Nusselt number is the product of film coefficient and hydraulic diameter divided by coolant thermal conductivity. Decreasing channel thickness reduces hydraulic diameter nearly proportionately. Thus, reducing channel thickness increases the film coefficient, which, in turn, reduces the film temperature rise.

Two perturbed PLTEMP/ANL cases were used to study the effect of channel thickness on clad surface temperature. In one the channel thickness was reduced by 8 mils – 4 mils for each half channel – and in the other it was increased by 8 mils. In the base case and the two perturbed cases the 25-inch channel length is divided into three vertical regions with a $7/8^{th}$ inch length at the inlet and outlet and a 23.25-inch length in the fueled region. Only the thickness of the 23.25-inch length was perturbed. In the perturbed cases, the 0.5 inlet and outlet K-loss associated with the fuel assembly were assigned to the fueled length rather than to the inlet or the outlet. These steps were taken so that the K-loss of 7 associated with the inlet piping would in all three cases be associated with the unperturbed channel thickness, as it should be, and the 0.5 channel inlet and outlet K-losses would be associated with the fueled channel thickness of each model.

As in the other perturbed cases, the small increase or decrease in channel flow causes a small increase or decrease in the flow and pressure drop associate with the inlet piping. However, these changes should not occur because there should be essentially no change in the total reactor flow due to one of many channels being 6 mils from its nominal thickness. Thus, there is a slight, but acceptable, error in the perturbed results which will be ignored.

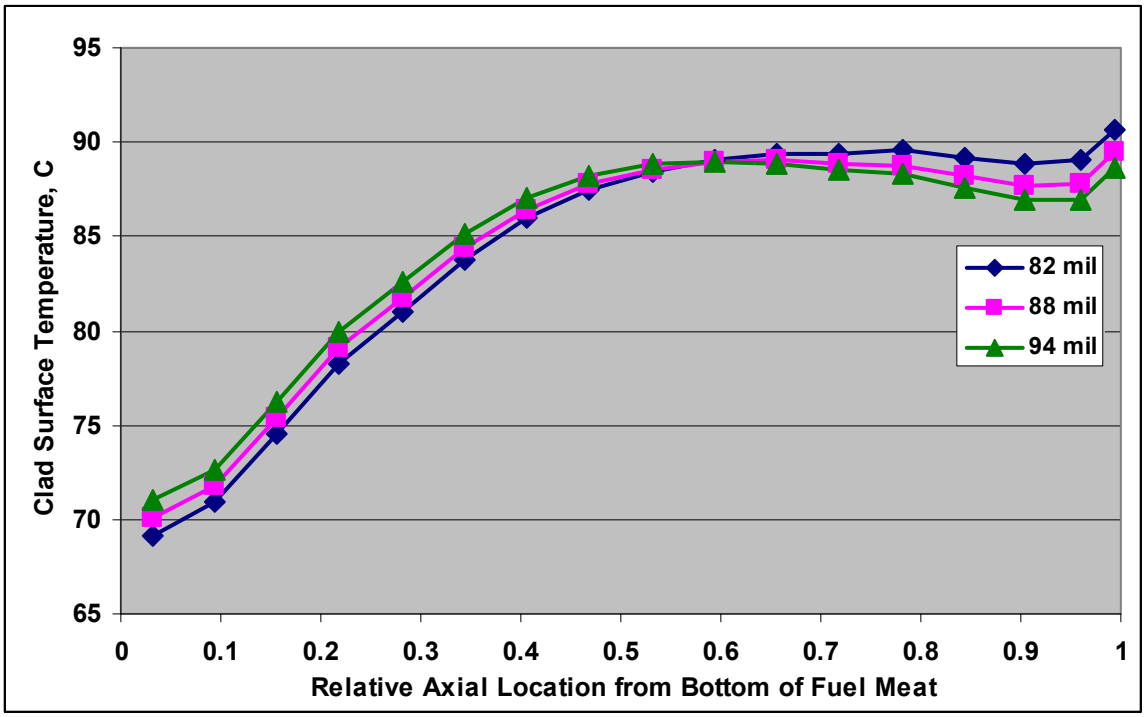

Figure 4.7-2 Axial Distributions of Clad Surface Temperature for Hottest Channel at 200 kW for Minimum, Nominal, and Maximum Channel Thicknesses (This includes only the hot channel factor for the global film coefficient.)

Figure 4.7-2 shows the axial distribution of clad surface temperature for the unperturbed, 88-mil, case and the two perturbed cases. Onset of nucleate boiling occurs when the clad surface temperature is about 2 degrees Celsius above the local coolant saturation temperature. The clad temperature is rather uniform over the upper half of the channel because, as Figure 4.6-5 shows, the heat flux drops off dramatically over the upper half of the fuel length. Thus, as the bulk coolant temperature is increasing the film temperature rise is decreasing. As can be seen from Figure 4.7-2, the peak clad surface temperature differs by only a few degrees among the three cases. The temperature increase from the bulk coolant inlet temperature of 54.44° C to the peak clad surface temperature is 36.16, 35.00, and 34.56° C for the 82, 88, and 94 mil cases, respectively. Thus, the most limiting case is the 82 mil case and the least limiting is the 94 mil case. The ratio of the largest temperature rise to the one for the unperturbed case is 36.16/35.00 = 1.033. One option would be to use this value for both F_{bulk} and F_{film} of the channel spacing uncertainty. A perhaps better approach was chosen in which F_{bulk} is determined from the unperturbed and 82-mil perturbed cases and the beneficial effect on the film temperature rise is ignored.

For the unperturbed case, as indicate earlier, the bulk coolant temperature rise from the inlet to the exit is 27.066° C. For the perturbed 82-mil case the corresponding temperature rise is 28.786° C. Thus, for an 8-mil decrease in channel thickness, the value for F_{bulk} is 28.786/27.066 = 1.064. It is no coincidence that this also essentially corresponds to the decrease in combined flow rate for the two half channel of 8.4960×10^{-3} kg/s to 7.9893×10^{-3} kg/s, i.e., $8.4960 \times 10^{-3} / 7.9893 \times 10^{-3} = 1.063$. Since the power is the same for both cases, the product of the flow rate

and the bulk coolant temperature rise should also be the same for both cases. The very slight difference between 1.064 and 1.063 can be attributed to difference in round-off error. Thus, F_{bulk} and F_w for the channel spacing uncertainty are both set to 1.064 in Table 4.7-2. The beneficial effect on film temperature rise is ignored and F_{film} is set to 1.00.

As in the analysis of the force-flow hot channel factors, the random errors are statistically combined and the result is indicated in red in the hot channel factor table. The product of the random and the systematic errors are also included in the hot channel factor table although they are not directly used in the analysis.

4.7.4.6 Results with Hot Channel Factors Included

The random errors combined hot channel factors specified in Table 4.7-2 for F_q, F_{bulk}, and F_{film} were included in the above NatConv_RI_200kW_03b.inp base case model and the built-in search for the power at which the onset of nucleate boiling is predicted to occur was activated. The new model was named NatConv_RI_200kW_03f.inp and is listed in Figure 4.7-3. The channel power at which onset of nucleate boiling was predicted is 1.7812 kW. This is the hottest channel for which the channel power is 0.9653 kW when the reactor power is 200 kW. Therefore, 1.7812 kW corresponds to a reactor power of 1.7812 / 0.9653 × 200 kW = 369 kW. For this limiting case the channel flow rate is 1.150×10^{-2} kg/s, which is 35% greater than the corresponding case NatConv_RI_200kW_03b.inp channel flow rate for which the reactor power is assumed to be 200 kW and F_q, F_{bulk}, and F_{film} are each 1.0. The large flow increase occurs because with increased power comes increased bulk coolant temperature which increases the buoyancy and reduces the coolant viscosity and the resistance to flow.

4.7.4.7 Effect of Doubling the Inlet Piping K-Loss Value and Also of Reducing it to Zero

Although the K-loss value of 7 being assumed for the piping leading from the coolant header gate to the reactor inlet plenum is believed to a conservatively large value, it is helpful to know the sensitivity of the predicted 369 kW allowed power to this K-loss value. Therefore, the analysis was repeated with the K-loss value of 7 for the inlet piping doubled to 14, making the inlet K-loss in the model 14.5 instead of 7.5. The channel power at which onset of nucleate boiling occurred decreased from 1.7812 kW to 1.6991 kW. The corresponding reduced reactor power is 1.6991 / 0.9653 × 200 kW = 352 kW. This represents a 4.6% reduction in allowed power. The analysis was also performed with the assumed K-loss value of 7 for the inlet piping reduced to 0, making the inlet K-loss in the model 0.5 instead of 7.5. The channel power at which onset of nucleate boiling occurred increased from 1.7812 kW to 1.8951 kW. The corresponding increased reactor power is 1.8951 / 0.9653 × 200 kW = 393 kW. This represents a 6.5% increase in allowed power. Thus, the allowed power is relatively insensitive to the uncertainty in inlet piping hydraulic resistance.

4.7.5 Verification of Key Results

In the analysis of forced-flow behavior in Section 4.6 it was possible to determine the channel flow rate by an independent means because the flow rate was not tightly coupled to the channel bulk coolant temperatures. Given the flow rate it was possible to verify key PLTEMP/ANL

```
RINSC, 88 mil channel, 1 internal plate; NC; 200 kW   Hottest Plate; All HCF's  0100
   5   0   6   1   0       1   1   0   0   0   0   0   0   2   1   0   0   0   00200
          1.          1.          1.2                                           0201
!  4       0.001       0.003   1          1.0                                   0203
   1   3       0.001          1.           1.          1.   0   0               30300-1
        1.07        1.23        1.23                                           0300A-1
   1   2          1.                                                           0301-1
   1   1   1                                                                   0302-1
     1.32483                                                                   0303-1
!         1.          1.          0.          0.                              0304-1
!         1.          1.     0.59055          0.    0.066548   0.0022352        0304-1
!         1.          1.          0.          0.                              0304-1
! total fuel plate length = 25", 23.25" fueled & 1.75/2 = 0.875" unfueled - each end
! Use a K = 0.5 at each end for channel inlet and outlet
! Increase K at the inlet by 10 to account for inlet duct resistance
! The K at the inlet of 10 to account for duct resistance was reduced to 7 to
! ,,, to account for difference between the velocity of the hottest channel and
! ... average core velocity, which is ~equal to the maximum duct velocity.
   14.870e-5    4.325e-3    0.022225         7.5    0.066548   0.0022352        0304-1
   14.870e-5    4.325e-3     0.59055          0.    0.066548   0.0022352        0304-1
   14.870e-5    4.325e-3    0.022225         0.5    0.066548   0.0022352        0304-1
          0.          0.          0.                                           0305-1
! channel length (fueled portion)=23.25"=0.59055 m, total width=2.62"=0.066548 m,
!   and thickness=0.088"=0.0022352 m
! plate fueled width=2.395"
! channel unfueled width (each side)=(2.62"-2.395")/2=0.1125"=2.8575e-3 m
! clad thickness =0.015"=3.81e-4 m; meat thickness=0.020"=5.08e-4 m
   2   3   2.8575e-3     0.59055     3.81e-4          0.     5.08e-4         40.0306-1
! Assume thickness=0.088"; 1/2 channel on each side of plate
    7.435e-5    4.325e-3      0.0688          0.    0.066548   0.0022352        0307-1
    7.435e-5    4.325e-3      0.0688          0.    0.066548   0.0022352        0307-1
    0.066548                                                                   0308-1
          1.                                                                   0309-1
!       0.17          0.        0.17        0.01       46.11          0.        0500
!         0.          0.                                                       0500
! 9.653 kW ==> 2.0 MW;  Thus, 200 kW = 0.2 MW = 0.2 * (9.653/2000) MW = 9.6530e-4 MW
! 130 F = 54.44 C
      8.0e-6          0.          0.   1.7813e-3       54.44       0.175        0500
          0.          0.                                                       0500
  0      0.0001        32.5          0.          0.                            0600
! Equilibrium Core, Assembly D6, Plate 1
! This axial power shape has been inverted so that 0 corresponds to the bottom.
 -18                                                                           0700
     0.00000     0.03125     0.99993                                           0701
     0.06250     0.09375     1.00578                                           0701
     0.12500     0.15625     1.12725                                           0701
     0.18750     0.21875     1.24832                                           0701
     0.25000     0.28125     1.28940                                           0701
     0.31250     0.34375     1.32483                                           0701
     0.37500     0.40625     1.31201                                           0701
     0.43750     0.46875     1.25813                                           0701
     0.50000     0.53125     1.17284                                           0701
     0.56250     0.59375     1.07059                                           0701
     0.62500     0.65625     0.95889                                           0701
     0.68750     0.71875     0.84137                                           0701
     0.75000     0.78125     0.74583                                           0701
     0.81250     0.84375     0.62614                                           0701
     0.87500     0.90357     0.52769                                           0701
     0.93214     0.96072     0.48115                                           0701
     0.98929     0.99464     0.56185                                           0701
     1.00000                                                                   0701
  0                                                                            0702
```

Figure 4.7-3 – PLTEMP/ANL V4.0 Input for Onset of Nucleate Boiling Predictions for Natural-Convective Flow

predictions with hand calculations. In the PLTEMP/ANL analysis of natural-convective flow, on the other hand, the buoyancy-driven channel flow rate is tightly couple to the bulk coolant temperatures. If the flow were known, it would be possible to verify key PLTEMP/ANL predictions with hand calculations, as was done for the forced-convection analysis. Since the buoyancy-driven flow is the new element here, there is a need to show that the PLTEMP/ANL predictions of natural convective flow are fundamentally correct. Another key difference in the current analysis is that the channel flow is laminar instead of turbulent. A consequence of this is the calculation of Nusselt number, which is needed to determine film coefficient, is different. Thus, the two items to be verified are 1) the natural-convective flow rate and 2) the film coefficient.

The buoyancy driven flow rate can be determined by equating the buoyancy pressure rise over the length of the heated channel with the pressure drop due to friction and K-losses. The buoyancy driven pressure rise is the product of the acceleration due to gravity (9.81 m/s^2) and integral of the density difference over the length of channel (i.e., $\int_0^L \Delta\rho \, dx$), where $\Delta\rho$ is the difference between the tank coolant density and the local density of the bulk coolant, and L is the length of the channel. The average density over a length can be estimate as the density corresponding to the average temperature over the length. The bulk coolant temperature distribution predicted by case NatConv_RI_200kW_03f.inp was copied to a computer spreadsheet and numerically integrated to determine that the average temperature over the 23.25-in fuel meat length was 75.0° C. The coolant temperature of the 7/8th-inch length between the top of the fuel meat and the channel exit was 91.2° C. These temperatures do not include hot channel factors because the increase in bulk coolant temperature due to the F_{bulk} hot channel factor is not part of the flow calculation in the PLTEMP/ANL code.

Table 4.7-3 lists essential quantities used in the verification. As the table shows, the estimate of the buoyancy pressure is 68.99 Pa. This pressure rise is based on the coolant densities at 54.44, 75.0, and 91.2° C and the 23.25-inch and 7/8th-inch lengths. The sum of the friction and K-loss pressure drops, as described in equation (1) below, are equated to the 68.99 Pa value to obtain the flow rate. For all of the verification calculations the water properties are obtained from the the 1996 NIST/ASME Steam Tables for a pressure of 1.75 bar.

The sum of the friction and K-loss pressure drops are given by the following:

$$\Delta P = \frac{\dot{m}^2}{2 A^2}\left(\frac{K_{in}}{\rho_{in}} + f\frac{L}{D} + \frac{K_{out}}{\rho_{out}}\right) \qquad (1)$$

Here $\dot{m}$ is the channel flow rate that is being sought, A is the flow area of the channel, K_{in} is the inlet K-loss, which is 7.5, K_{out} is the outlet K-loss, which is 0.5, ρ_{in} is the coolant density at the inlet, ρ_{out} is the coolant density at the out, f is the friction factor, L is the channel length, which is taken to be 25.0 inches, and D is the hydraulic diameter of the channel.

Another equation is needed to determine the friction factor. For laminar flow, f = C / Re, where C is a constant and Re is the Reynolds number. The Reynolds number can be shown to be

$4\dot{m}/(\mu P_w)$, where μ is the coolant viscosity and P_w is the channel wetted perimeter. Since viscosity varies with temperature over the length of the channel, the PLEMP/ANL code in effect calculates $f \times \Delta L$ for each axial layer of the model and uses the sum of all of the $f \times \Delta L$'s over the length of the channel to represent the $f \times L$. For the current estimate, f evaluated at the average temperature over the 23.25-inch fuel meat length, which is 75.0° C, will be assumed to apply to the entire 25-inch channel length. The constant C is 96 for a channel formed between two infinitely wide parallel plates. For the channel under consideration, the thickness is 0.088 inches and the width is 2.62 inches, yielding an aspect ratio of 0.033588. Based on equation (3.158) in Reference 2, C increased by a factor of 4 to obtain the Moody rather than the Fanning friction factor, is 91.8.

The values of the quantities used to solve equation (1) are shown in Table 4.7-3. Equation (1) was solved with the aid of a computer spreadsheet to obtain a value of 0.011267 kg/s for $\dot{m}$. This is 98.0% of the 0.011498 kg/s predicted by the PLTEMP/ANL code.

In the output for PLTEMP/ANL case NatConv_RI_200kW_03f.inp a film coefficient of 935.4 W/m^2-K was provide for a bulk coolant temperature of 75.1° C. The bottom part of Table 4.7-3 shows key values from the hand-calculation of film coefficient. The Nusselt number of 7.63 was multiplied by the thermal conductivity of water at 75.1° C and divided by the product of the hydraulic diameter and the 1.2 global hot channel factor to yield a film coefficient of 980.4 W/m^2-K. This value is only 4.8% greater than the PLTEMP/ANL value.

4.7.6 Summary and Conclusions

For the analysis of the reactor in natural-convective mode, the safety limiting inlet temperature of 130° C and water depth of 23.54 feet above the active core were used even though these are more restrictive than the corresponding LSSS values. They hydraulic resistance along the inlet flow path from the coolant header gate to the lower plenum, as indicated by the red arrows in Figure 4.7-2, was included in the analysis and is represented by a K-loss value of 7 at the inlet to the limiting coolant channel.

The PLTEMP/ANL code was used in the analysis. Only the limiting fuel plate was modeled. The model consisted of a single fuel plate cooled on each side by half of a 0.088-inch thick coolant channel. Thus, the power of the fuel plate was assumed to be removed by two channels that are each 0.044-inch thick and have the hydraulic diameter of a 0.088-inch thick channel. Hot channel factors were determine and are as shown in Table 4.7-2 and are included in the analysis.

In the Section 4.6 analysis of force-convective flow, key quantities associated with the PLTEMP/ANL determination of the margin to onset of nucleate boiling were verified via hand calculations. Since natural-convective flow requires the determination of both the buoyancy-drive flow rate and the film coefficient for laminar flow conditions, additional hand calculations were performed to show that the flow rate and a film coefficient predicted by the PLTEMP/ANL model for the current analysis are close to their expected values.

The analysis shows that onset of nucleate boiling will occur at 369 kW with all uncertainties included. This is to be compared with the nominal power for the natural-convective mode of 100 kW, the LSSS value of 115 kW, the LSSS value when a 10-kW power measurement uncertainty is included of 125 kW, and the safety limit value of 200 kW.

In conclusion, the RINSC reactor can be safely operated in the natural-convective mode at a measured power of 100 kW.

References:

1. I. E. Idelchik, *Handbook of Hydraulic Resistance*, Second Edition, Hemisphere Publishing Corporation, New York, 1986.

2. Sadic Kakac, Ramesh K. Shah, Win Aung, *Handbook of Single-Phase Convective Heat Transfer*, John Wiley and Sons, New York, 1987.

Table 4.7-3 Verification of PLTEMP/ANL Flow Rate and Film Coefficient

Item	Value
inlet temp, C	54.44
inlet density, kg/m^3	986.0
avg Tbulk over fuel, C	75.0
density avg Tbulk, kg/m^3	974.9
fuel meat length, in	23.25
exit Tbulk, C	91.2
exit density, kg/m^3	964.5
exit length, in	0.875
gravitational acceleration, m/s^2	9.81
buoyancy presssure rise, Pa	68.99
flow rate, kg/s	0.011267
duct length, in	25
duct width, in	2.62
duct thickness, in	0.088
duct area, m^2	0.0001487
Kin	7.5
Kout	0.5
duct length, m	0.635
avg viscosity, Pa-s	0.0003774
wetted perimeter, m	0.1375664
duct hydraulic diameter, m	0.004325
avg Reynolds number	868.1
fRe	91.8
friction factor	0.1058
friction factor * Length / Diam.	15.5
friction pressure drop, Pa	68.99
PLTEMP/ANL flow rate, kg/s	0.011498
ratio of calc to PLTEMP flow	0.9799
Nusselt number	7.63
hot channel factor	1.2
thermal cond. @ 75.1 C, W/m-K	0.6669
film coef., W/m^2-K	980.4
PLTEMP film coef., W/m^2-K	935.4
ratio of calculate-to-PLTEMP film	1.048